

## Temperature-Dependent Coordination of Phosphine to Five-Coordinate Alkenylruthenium Complexes

Sripriya K. Seetharaman,<sup>†</sup> Min-Chul Chung,<sup>‡</sup> Ulrich Englisch,<sup>§</sup> Karin Ruhlandt-Senge, and Michael B. Sponser\*

Department of Chemistry, Syracuse University, Syracuse, New York 13244-4100

Received July 25, 2006

The red, five-coordinate complexes  $\text{Ru}(\text{CO})\text{Cl}(\text{PPh}_3)_2(\text{CH}=\text{CHPh})$  and  $[\text{Ru}(\text{CO})\text{Cl}(\text{PPh}_3)_2(\mu\text{-CH}=\text{CHC}_6\text{H}_4\text{CH}=\text{CH})]$  undergo reversible coordination of  $\text{PPh}_3$  at low temperature to produce the pale yellow, six-coordinate complexes  $\text{Ru}(\text{CO})\text{Cl}(\text{PPh}_3)_3(\text{CH}=\text{CHPh})$  and  $[\text{Ru}(\text{CO})\text{Cl}(\text{PPh}_3)_3(\mu\text{-CH}=\text{CHC}_6\text{H}_4\text{CH}=\text{CH})]$ . X-ray crystal structures of the latter complex and of the hydride complex  $\text{RuH}(\text{CO})\text{Cl}(\text{PPh}_3)_3$  were obtained.  $^1\text{H}$  and  $^{31}\text{P}$  NMR spectra between 20 and  $-70$  °C exhibit large changes in both equilibrium constants and dynamic effects. Thermodynamic parameters,  $\Delta H = -17.5 \pm 2.0$  kcal/mol and  $\Delta S = -57.5 \pm 7.6$  eu, were obtained for  $\text{PPh}_3$  coordination to the monoruthenium complex, and activation parameters,  $\Delta H^\ddagger = 20.6 \pm 0.7$  kcal/mol and  $\Delta S^\ddagger = 41.6 \pm 2.0$  eu, were obtained for the reverse decoordination. Coordination of  $\text{PPh}_3$  was not observed upon cooling of the shorter bridged complex,  $[\text{Ru}(\text{CO})\text{Cl}(\text{PPh}_3)_2(\mu\text{-CH}=\text{CHCH}=\text{CH})]$ .

### Introduction

As shown by many literature examples, addition of the six-coordinate ruthenium hydride  $\text{RuH}(\text{CO})\text{Cl}(\text{PPh}_3)_3$  to alkynes affords five-coordinate *E*-alkenyl complexes of the type  $\text{Ru}(\text{CO})\text{Cl}(\text{PPh}_3)_2(\text{R}^1\text{C}=\text{CHR}^2)$ .<sup>1–3</sup> The steric bulk of the alkenyl ligand, despite being trans to the open coordination site, apparently leaves too little room for coordination of the third triphenylphosphine ligand (cone angle 145°).<sup>4</sup> A variety of smaller ligands, such as isocyanides, pyridines, and carbon monoxide, do coordinate to the alkenyl complexes to give six-coordinate, octahedral complexes.<sup>2,3,5</sup> With the larger phosphine *P*-*i*-Pr<sub>3</sub> (cone angle 160°), even the hydride complex is five-coordinate ( $\text{RuH}(\text{CO})\text{Cl}(\text{P-}i\text{-Pr}_3)_2$ ),

as are the alkenyl complexes formed from it,<sup>6</sup> though small ligands can still coordinate.<sup>7</sup> With the smaller  $\text{PMe}_3$  (cone angle 118°), six-coordinate alkenyl complexes,  $\text{Ru}(\text{CO})\text{Cl}(\text{PMe}_3)_3(\text{R}^1\text{C}=\text{CHR}^2)$ , are common, generally formed by treatment of  $\text{Ru}(\text{CO})\text{Cl}(\text{PPh}_3)_2(\text{R}^1\text{C}=\text{CHR}^2)$  with  $\text{PMe}_3$ .<sup>8</sup>

We have observed that the five-coordinate alkenyl complex  $\text{Ru}(\text{CO})\text{Cl}(\text{PPh}_3)_2(\text{CH}=\text{CHPh})$  (**1**) can accept an additional  $\text{PPh}_3$  ligand at low temperature, as shown by the equilibrium equation in Scheme 1, to produce the saturated  $\text{Ru}(\text{CO})\text{Cl}(\text{PPh}_3)_3(\text{CH}=\text{CHPh})$  (**1-P**).<sup>9</sup> This coordination is readily observable, as a red  $\text{CH}_2\text{Cl}_2$  solution of **1** and  $\text{PPh}_3$  becomes pale yellow upon cooling to  $-78$  °C. Warming the solution again to room temperature returns the red color. The coordination, being enthalpically favorable (negative  $\Delta H$ ) and entropically unfavorable (negative  $\Delta S$ ), should indeed

\* To whom correspondence should be addressed. E-mail: sponser@syr.edu.

<sup>†</sup> Current address: Lawrence University, Appleton, WI.

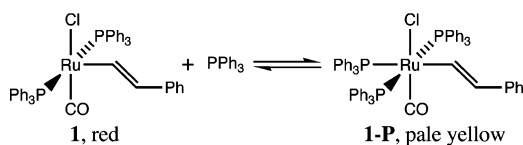
<sup>‡</sup> Current address: Sunchon National University, Sunchon, Republic of Korea.

<sup>§</sup> Current address: Cornell University, Ithaca, NY.

- (1) Torres, M. R.; Vegas, A.; Santos, A. *J. Organomet. Chem.* **1986**, *309*, 169–177.
- (2) Santos, A.; Lopez, J.; Gonzalez, J. J.; Tinoco, P.; Echavarren, A. M. *Organometallics* **1997**, *16*, 3482–3488.
- (3) Romero, A.; Santos, A.; Lopez, J.; Echavarren, A. M. *J. Organomet. Chem.* **1990**, *391*, 219–223.
- (4) Davila, R. M.; Staples, R. J.; Elduque, A.; Harlass, M. M.; Kyle, L.; Fackler, J. P. *J. Inorg. Chem.* **1994**, *33*, 5940–5945.
- (5) Rickard, C. F. E.; Roper, W. R.; Woodgate, S. D.; Wright, J. L. *J. Organomet. Chem.* **2000**, *607*, 27–40.
- (6) Esteruelas, M. A.; Werner, H. J. *J. Organomet. Chem.* **1986**, *303*, 221–231.

- (7) Buil, M. L.; Esteruelas, M. A.; Goni, E.; Olivan, M.; Onate, E. *Organometallics* **2006**, *25*, 3076–3083.
- (8) Yin, J.; Yu, G.; Guan, J.; Mei, F.; Liu, S. H. *J. Organomet. Chem.* **2005**, *690*, 4265–4271.
- (9) A recent report (Lam, T. C. H.; Mak, W.-L.; Wong, W.-L.; Kwong, H.-L.; Sung, H. H. Y.; Lo, S. M. F.; Williams, I. D.; Leung, W.-H. *Organometallics* **2004**, *23*, 1247–1252) claims to use **1-P** as a room-temperature-stable reactant, but the complex used was presumably **1**. The complex is described as orange and was prepared by the method of ref 1, which reports **1** but not **1-P**.
- (10) Xia, H.; Wen, T. B.; Hu, Q. Y.; Wang, X.; Chen, X.; Shek, L. Y.; Williams, I. D.; Wong, K. S.; Wong, G. K. L.; Jia, G. *Organometallics* **2005**, *24*, 562–569.
- (11) Ahmad, N.; Levison, J. J.; Robinson, S. D.; Uttley, M. F. *Inorg. Synth.* **1974**, *15*, 45–64.

Scheme 1



be preferred at lower temperatures. The corresponding osmium complex,  $\text{Os(CO)Cl(PPh}_3\text{)}_3(\text{CH=CHPh})$ , has recently been reported to be stable at room temperature.<sup>10</sup>

In this paper, we report NMR studies on the coordination of  $\text{PPh}_3$  to **1** and related complexes. Variable temperature  $^{31}\text{P}$  and  $^1\text{H}$  spectra have been recorded and analyzed with respect to both thermodynamic and kinetic aspects of the reaction. This is a rare study that provides both types of parameters from the same data—made more difficult by the fact that coalescence phenomena obscured a good portion of the equilibrium data. The quantitative results are valuable additions to the limited literature of experimentally determined phosphine binding parameters. Our study also included two diruthenium complexes with different bridging ligands that affect the steric demands and coordination behavior. An X-ray crystal structure of a  $\text{PPh}_3$  adduct  $[\text{Ru(CO)Cl(PPh}_3\text{)}_3]_2(\mu\text{-CH=CHC}_6\text{H}_4\text{CH=CH})$  (**2-P<sub>2</sub>**) helps to confirm the nature of the coordination process and the steric environment in the complexes.

## Experimental Section

All sample manipulations were carried out under a dinitrogen atmosphere in a glove box. Solvents were either degassed (diethyl ether) or purified by distillation or vacuum transfer from  $\text{CaH}_2$  (pentane,  $\text{CH}_2\text{Cl}_2$ , and  $\text{CD}_2\text{Cl}_2$ ).  $\text{RuH(CO)Cl(PPh}_3\text{)}_3$ ,<sup>11</sup>  $\text{Ru(CO)Cl(PPh}_3\text{)}_2(\text{CH=CHPh})$  (**1**), and  $[\text{Ru(CO)Cl(PPh}_3\text{)}_2]_2(\mu\text{-CH=CHC}_6\text{H}_4\text{CH=CH})$  (**2**) were prepared according to the reported procedures. Commercial triphenylphosphine was used without purification.

$^1\text{H}$  and  $^{31}\text{P}$  NMR spectra were recorded on a Bruker DPX-600 at seven different temperatures: 20, 5,  $-10$ ,  $-25$ ,  $-40$ ,  $-55$ , and  $-70$  °C for two samples containing **1** and a slight excess of  $\text{PPh}_3$  in  $\text{CD}_2\text{Cl}_2$  (sample 1 under air and sample 2 under vacuum). For samples 1 and 2, the peaks obtained at temperatures ranging from 20 to  $-40$  °C were taken as averaged peaks representing mixtures of **1**,  $\text{PPh}_3$ , and **1-P**. After verification that the weighted-average method would be accurate, the relative amounts of **1**,  $\text{PPh}_3$ , and **1-P** at each temperature were calculated by weighted-average interpolation relative to the chemical shifts and coupling constants obtained for the pure components.<sup>14</sup> The equilibrium constants for the coordination process at each temperature were then computed and used to create van't Hoff plots. The chemical shifts and coupling constants from which the thermodynamic data were calculated are given in the Supporting Information, along with more detailed descriptions of the methods used. NMR line-shape fitting was carried out using the programs SwaN-MR (version 3.6.1)<sup>15,16</sup> and MEXICO (version 3.0).<sup>17–19</sup>

(12) Santos, A.; Lopez, J.; Montoya, J.; Noheda, P.; Romero, A.; Echavarren, A. M. *Organometallics* **1994**, *13*, 3605–3615.

(13) Jia, G.; Wu, W. F.; Yeung, R. C. Y.; Xia, H. P. *J. Organomet. Chem.* **1997**, *539*, 53–59.

(14) London, R. E. *J. Magn. Reson., Ser. A* **1993**, *104*, 190–196.

(15) Balacco, G. *J. Chem. Inf. Comput. Sci.* **1994**, *34*, 1235–1241.

(16) A newer program by the same author is available: Balacco, G. <http://www.inmr.net>.

(17) Bain, A. D. <http://www.chemistry.mcmaster.ca/bain/exchange.html>.

## X-ray Crystallography of $\text{RuH(CO)Cl(PPh}_3\text{)}_3$ and **2-P<sub>2</sub>**

Crystallographic data were collected with a Bruker P4 diffractometer equipped with a SMART CCD system<sup>20</sup> and using Mo  $\text{K}\alpha$  radiation ( $\lambda = 0.71073$  Å). The data were corrected for Lorentz and polarization effects. Absorption corrections were made using SADABS.<sup>21</sup> The structure solution and refinement were carried out using the SHELX97<sup>22</sup> crystallographic software package. The structure was solved using direct methods. After location of all the non-hydrogen atoms, the model was refined against  $F^2$ , initially using isotropic then anisotropic thermal displacement parameters.

Crystals of  $\text{RuH(CO)Cl(PPh}_3\text{)}_3$  were grown from pentane/ $\text{CH}_2\text{Cl}_2$ . The crystals were transferred under a stream of  $\text{N}_2$  into a Petri dish filled with a highly viscous hydrocarbon oil (Infinium). With the aid of a microscope, a crystal was attached to the end of a glass fiber and mounted in the cold  $\text{N}_2$  stream in the diffractometer.

$\text{RuH(CO)Cl(PPh}_3\text{)}_3$  was found to be a merohedral twin. In complete analogy to the isostructural structure for  $\text{OsH(CO)Cl(PPh}_3\text{)}_3$ ,<sup>10</sup> systematic absences for a 3<sub>1</sub> and a 3<sub>2</sub> axis were detected. It was found that the 2-fold axis was not a true crystallographic one, and after interchanging  $h$  and  $k$  and reversing  $l$  (010 100 00 1), the structure was refined in the space group  $P3_1$  to complete satisfaction. An earlier structure report on  $\text{RuH(CO)Cl(PPh}_3\text{)}_3$  contains the structural refinement of the compound in the space group  $P3_2$  with  $R_1$  of 9.40% with the phenyl ring positions constrained to ideal hexagons. In our case, the  $R_1$  value dropped to 3.31%, and estimated standard deviations (esd's) for the atomic positions and displacement parameters improved significantly, allowing the independent refinement of all molecular components.

Crystals of **2-P<sub>2</sub>** were grown by slow diffusion over 2 weeks at  $-78$  °C from a  $\text{CH}_2\text{Cl}_2$  solution of **2** and 2 equiv of  $\text{PPh}_3$  over which was layered 4 volumes of a 20:1 mixture of pentane and THF. The nearly colorless crystals quickly turned orange upon warming to room temperature, making it necessary to keep the crystals below  $-30$  °C at all times. Moreover, removal of the crystals from the mother liquor resulted in immediate solvent loss and destruction of the crystals. The use of the hydrocarbon oil was hampered by its low-temperature viscosity. With a microscope positioned next to the diffractometer, a few crystals in mother liquor were quickly transferred into a Petri dish containing a few milliliters of diethyl ether cooled with dry ice. A crystal was then mounted at the end of a grease-tipped fiber and quickly moved into the stream of cold  $\text{N}_2$  gas (transfer time ca. 2 s) on the diffractometer.

Compound **2-P<sub>2</sub>** was found to contain a large number of lattice solvent molecules, explaining the immediate desolvation upon removal of the mother liquor. Mounting from cooled diethyl ether ( $-78$  °C) prevented desolvation, while avoiding the decomposition of the crystals observed upon decoordination of  $\text{PPh}_3$ . Some solvents of crystallization were found to be disordered. The positions were refined using split parameters as well as restraints.<sup>22</sup> Two solvent molecules, one  $\text{CH}_2\text{Cl}_2$  and one THF, could not be refined satisfactorily and were removed from the refinement using the squeeze function in PLATON.<sup>23</sup>

(18) Bain, A. D.; Rex, D. M.; Smith, R. N. *Magn. Reson. Chem.* **2001**, *39*, 122–126.

(19) Bain, A. D.; Duns, G. J. *Can. J. Chem.* **1996**, *74*, 819–824.

(20) SMART, Data Collection Software, version 4.050; Siemens Analytical Instruments, Inc.: Madison, WI, 1966.

(21) Sheldrick, G. M. SADABS: University of Göttingen: Göttingen, Germany, 1996.

(22) Sheldrick, G. M. SHELXTL-Plus: Program Package for Structure Solution and Refinement; Siemens Analytical X-Ray Instruments, Inc.: Madison, WI, 1999.

(23) Spek, A. L. In PLATON for Windows; Utrecht University: The Netherlands, 2000.

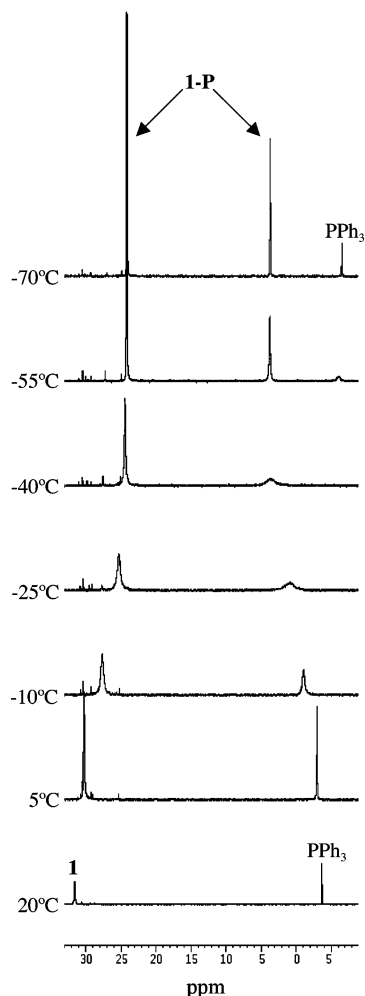


**Figure 1.** Temperature-dependent  $^{31}\text{P}$  NMR spectra of **1** and a slight excess of  $\text{PPh}_3$  in  $\text{CD}_2\text{Cl}_2$ .

Crystallographic data (excluding structure factors) for the two structures have been deposited with the Cambridge Crystallographic Data Center as supplementary publications 615733 ( $\text{RuH}(\text{CO})\text{Cl}(\text{PPh}_3)_3$ ) and 615734 (**2-P<sub>2</sub>**). Copies of these data can be obtained free of charge on application to CCDC, 12 Union Road, Cambridge CB21EZ, U.K. (fax: (+44) 1223-336-033; e-mail: deposit@ccdc.cam.ac.uk).

## Results and Discussion

**Coordination of Triphenylphosphine.**  $\text{Ru}(\text{CO})\text{Cl}(\text{PPh}_3)_2(\text{CH}=\text{CHPh})$  (**1**) was prepared from the reaction of  $\text{RuH}(\text{CO})\text{Cl}(\text{PPh}_3)_3$  with phenylacetylene.<sup>1</sup> The addition occurs with loss of  $\text{PPh}_3$  to give the five-coordinate complex. When the crude mixture, already containing 1 equiv of free phosphine, was cooled, a gradual and reversible color change was observed from red at ambient temperature to pale yellow at  $-78^\circ\text{C}$ .  $^{31}\text{P}$  and  $^1\text{H}$  NMR spectra recorded for clean mixtures of **1** and  $\text{PPh}_3$  between 20 and  $-70^\circ\text{C}$  (Figures 1 and 2) were consistent with the low-temperature coordination of  $\text{PPh}_3$  to give  $\text{Ru}(\text{CO})\text{Cl}(\text{PPh}_3)_3(\text{CH}=\text{CHPh})$  (**1-P**). In particular, the  $-70^\circ\text{C}$   $^{31}\text{P}$  spectrum showed a doublet at 23.9 ppm and a triplet at 3.4 ppm ( $J_{\text{PP}} = 15.3$  Hz) with an integration ratio of 2:1. Further evidence was obtained in the form of an X-ray crystal structure of a complex closely related to **1-P** (see below).

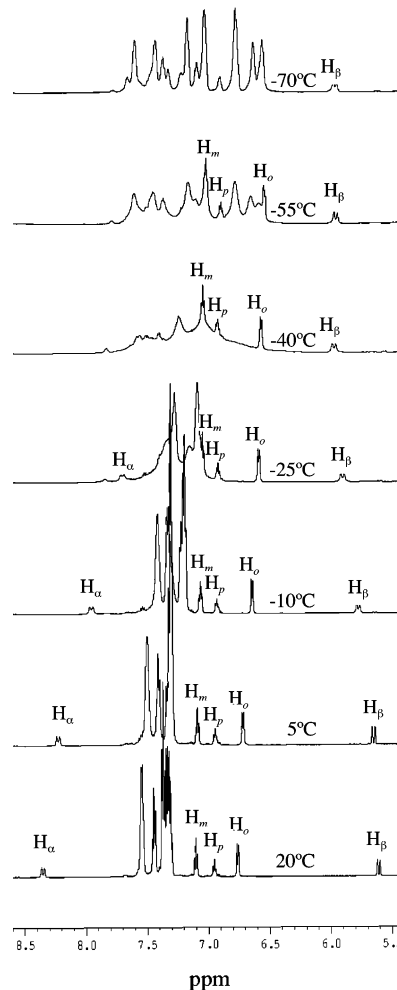
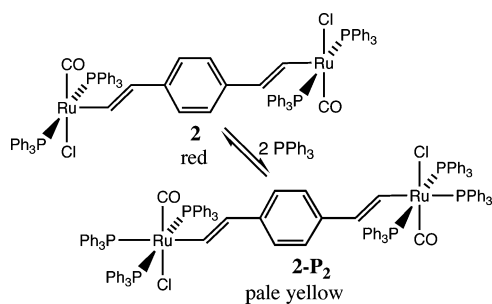


**Figure 2.** Temperature-dependent  $^1\text{H}$  NMR spectra of **1** and  $\text{PPh}_3$  in  $\text{CD}_2\text{Cl}_2$ .

The  $^{31}\text{P}$  NMR spectrum at  $-70^\circ\text{C}$  showed a mixture of **1-P** and excess  $\text{PPh}_3$  with no observable peak for **1**, indicating that the coordination equilibrium constant was very high at this temperature. As the temperature was raised, the peaks broadened, and the coordinated and free  $\text{PPh}_3$  peaks coalesced between  $-40$  and  $-25^\circ\text{C}$  to an averaged peak. The gradual upfield shift of the averaged peak between  $-25$  and  $20^\circ\text{C}$  (from  $-0.7$  to  $-4.1$  ppm) is consistent with an equilibrium shift away from **1-P** and toward **1** plus  $\text{PPh}_3$ . Likewise, the gradual downfield shift of the averaged peak representing the trans  $\text{PPh}_3$  ligands of **1** and **1-P** (from 25.4 to 31.5 ppm) over the same temperature range is also consistent with this equilibrium shift. The observation that the  $20^\circ\text{C}$  shifts (31.5 and  $-4.1$  ppm) do not quite match those observed for separate samples of **1** and  $\text{PPh}_3$  (31.6 and  $-4.6$  ppm) is consistent with an equilibrium that favors **1** and  $\text{PPh}_3$ , though not to the complete exclusion of **1-P**.

The series of  $^1\text{H}$  NMR spectra recorded at the same temperatures (Figure 2) is also interpretable in terms of the same coordination changes. The  $20^\circ\text{C}$  doublets at 8.36 and 5.60 ppm represent fast-exchange, averaged signals for the  $\alpha$ - and  $\beta$ -alkenyl hydrogens, respectively, coming close to the  $20^\circ\text{C}$  values for pure **1** (8.41 and 5.58 ppm). As the temperature was lowered, these signals shifted toward each other, with the  $\alpha$ -signal becoming lost in the  $\text{PPh}_3$  signals

Scheme 2

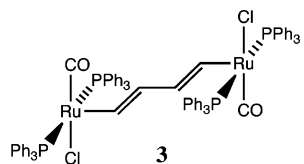


below  $-25\text{ }^{\circ}\text{C}$ . The  $\beta$ -signal, observable at all temperatures, broadened until  $-40\text{ }^{\circ}\text{C}$  and then sharpened again into a presumably slow-exchange doublet representing **1-P**. No doublet was observable at  $-70$  or  $-55\text{ }^{\circ}\text{C}$  for **1**, to be expected at 5.30 or 5.35 ppm, respectively, on the basis of spectra of pure samples of **1**.

The styryl phenyl signals in Figure 2 show smaller temperature-dependent shifts without broadening. The phosphine phenyl signals, in contrast, broadened as the temperature dropped to  $-25\text{ }^{\circ}\text{C}$  and then split into many signals over a large chemical shift range at  $-70\text{ }^{\circ}\text{C}$ . The large number of signals indicates that **1-P** must experience one or more types of restricted rotations, placing phenyl hydrogens in different and slowly exchanging environments. A very broad peak integrating for 1H was observed at 8.5 ppm in the  $-55$  and  $-70\text{ }^{\circ}\text{C}$  spectra, apparently representing a  $\text{PPh}_3$  hydrogen that resides in a particularly deshielded environment.

In a completely analogous fashion, coordination of  $\text{PPh}_3$  to the dinuclear complex **2** was also observed, ultimately producing **2-P<sub>2</sub>** (Scheme 2). Temperature-dependent solution colorations were essentially identical to those observed for Scheme 1. Spectral interpretations were somewhat complicated by the unsymmetrical nature of the intermediate **2-P**, but  $^{31}\text{P}$  and  $^1\text{H}$  spectral features were completely consistent with a stepwise coordination process.

Very interestingly, the dinuclear complex **3**,<sup>24</sup> with a shorter,  $\text{C}_4\text{H}_4$  bridging ligand, showed no evidence of  $\text{PPh}_3$  coordination, even at low temperatures. The color of a solution of **3** and  $\text{PPh}_3$  remained red when cooled to  $-78\text{ }^{\circ}\text{C}$ , and no qualitative changes were observed in the  $^{31}\text{P}$  or  $^1\text{H}$  NMR spectra between 20 and  $-70\text{ }^{\circ}\text{C}$ . The shorter bridge apparently brings the coordinated  $\text{PPh}_3$  ligands on the two Ru centers into close enough proximity that they are unable to bend away to accommodate an incoming  $\text{PPh}_3$  ligand.



An early report on the chemistry of  $\text{RuH}(\text{CO})\text{Cl}(\text{PPh}_3)_3$  claimed that the reaction with phenylacetylene produced either **1** or a pale yellow complex assigned the six-coordinate

Table 1. Crystal Data for  $\text{RuH}(\text{CO})\text{Cl}(\text{PPh}_3)_3$  and **2-P<sub>2</sub>**

	$\text{RuH}(\text{CO})\text{Cl}(\text{PPh}_3)_3 \cdot \text{CH}_2\text{Cl}_2$	<b>2-P<sub>2</sub></b> · 3 $\text{CH}_2\text{Cl}_2$ · 3THF
formula	$\text{C}_{56}\text{H}_{48}\text{Cl}_3\text{OP}_3\text{Ru}$	$\text{C}_{67.5}\text{H}_{64}\text{Cl}_4\text{O}_{2.5}\text{P}_3\text{Ru}$
fw	1036.27	1250.46
space group	$P3_1$	$C2/c$
<i>a</i> (Å)	12.5676(6)	26.803(2)
<i>b</i> (Å)	12.5676(6)	21.2043(15)
<i>c</i> (Å)	26.2720(17)	24.917(2)
$\alpha$ (°)	90	90
$\beta$ (°)	90	94.079(2)
$\gamma$ (°)	120	90
<i>V</i> (Å <sup>3</sup> )	3593.6(3)	14125(2)
<i>Z</i>	3	8
<i>T</i> (K)	95(2)	91(2)
<i>D</i> <sub>calc</sub> (g cm <sup>-3</sup> )	1.437	1.176
<i>R</i> ( <i>F</i> ) <sup>a</sup>	0.0331	0.0853
<i>R</i> <sub>w</sub> ( <i>F</i> ) <i>C</i>	0.0781	0.2032

$$^a R(F) = \frac{\sum ||F_o| - |F_c||}{\sum |F_o|}; R_w(F)C = \left[ \frac{\sum w(F_o^2 - F_c^2)^2}{\sum w(F_o^2)^2} \right]^{1/2}$$

Table 2. Selected Bond Lengths (Å) and Angles (deg) for  $\text{RuH}(\text{CO})\text{Cl}(\text{PPh}_3)_3$  and **2-P<sub>2</sub>**

$\text{RuH}(\text{CO})\text{Cl}(\text{PPh}_3)_3$		<b>2-P<sub>2</sub></b>	
Ru—Cl	2.499(1)	Ru—Cl	2.452(2)
Ru—P1	2.396(1)	Ru—P2	2.418(2)
Ru—P2	2.358(1)	Ru—P3	2.413(3)
Ru—P3	2.505(1)	Ru—P1	2.552(2)
Ru—C55	1.837(6)	Ru—C6	1.822(10)
C—O	1.141(6)	C—O	1.172(10)
		Ru—C1	2.073(8)
P1—Ru—P2	154.02(4)	P2—Ru—P3	159.99(8)
P1—Ru—P3	105.78(4)	P2—Ru—P1	98.61(8)
P2—Ru—P3	99.27(4)	P3—Ru—P1	100.67(8)
Cl—Ru—P3	99.11(4)	Cl—Ru—P1	98.80(8)
C55—Ru—P3	88.4(2)	C6—Ru—P1	85.0(3)
Ru—C55—O	178.9(5)	Ru—C6—O	178.5(7)
		C1—Ru—P2	81.4(2)
		C1—Ru—P3	80.2(2)
		C1—Ru—P1	172.4(2)
		C1—Ru—Cl	88.8(2)
		C1—Ru—C6	87.4(3)

alkenyl structure  $\text{Ru}(\text{CO})\text{Cl}(\text{PPh}_3)_3(\text{PhC}=\text{CH}_2)$ .<sup>1</sup> The former was prepared in  $\text{CH}_2\text{Cl}_2$  and the latter in  $\text{CH}_2\text{Cl}_2/\text{CH}_3\text{OH}$ . In our hands, only **1** was obtained in either solvent.

**X-ray Crystal Structures of  $\text{RuH}(\text{CO})\text{Cl}(\text{PPh}_3)_3$  and **2-P<sub>2</sub>**.** Although  $\text{RuH}(\text{CO})\text{Cl}(\text{PPh}_3)_3$  has been known since 1964 and has appeared in over 450 papers, its crystal structure has only been reported recently.<sup>25</sup> As mentioned above, the former data analysis did not recognize the merohedral twinning, resulting in nonsatisfactory data analysis and geometrical values. We here report an improved structure analysis (Tables 1 and 2).

The structure of  $\text{RuH}(\text{CO})\text{Cl}(\text{PPh}_3)_3$  (Figure 3) is very similar to that of the isostructural Os analogue; indeed, the twinning observed for this analogue was also observed for the Os congener. The isostructural relationship was found despite differences in solvent incorporation: one molecule of  $\text{CH}_2\text{Cl}_2$  in the Ru crystal vs one molecule of ethanol in the Os crystal. The unit cell parameters are slightly contracted for the Ru case, by 0.44% (*a* and *b*) and 0.20% (*c*), but the temperature for data collection was also lower (95 vs 295 K). The bond lengths to the metal atom (not including the

(24) Xia, H.; Yeung, R. C. Y.; Jia, G. *Organometallics* **1998**, *17*, 4762–4768.

(25) Snelgrove, J. L.; Conrad, J. C.; Yap, G. P. A.; Fogg, D. E. *Inorg. Chim. Acta* **2003**, *345*, 268–278.



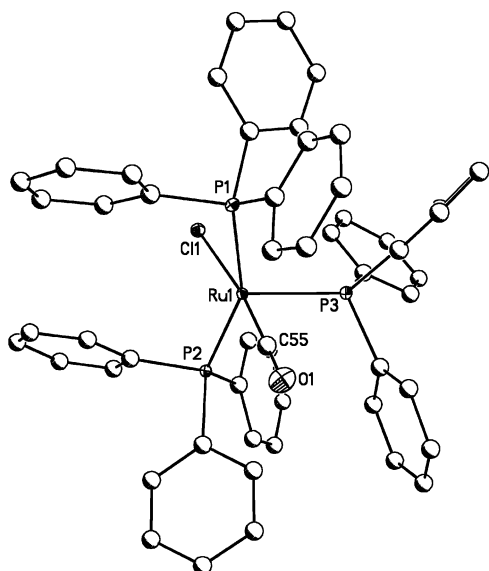


**Figure 3.** Molecular structure of  $\text{RuH}(\text{CO})\text{Cl}(\text{PPh}_3)_3$  with 30% thermal ellipsoids for non-carbon atoms. Hydrogen atoms have been omitted for clarity.

hydride, which was not found in either structure) vary by 1.5% or less, but the C–O distance is 6.3% longer in the Ru structure (1.141 vs 1.073 Å). Bond angles at the metal center differ by less than 2.6°, with a 4.7° difference for the M–C–O angle (178.9° vs 174.2°).

Differences with the previously reported structure for  $\text{RuH}(\text{CO})\text{Cl}(\text{PPh}_3)_3$ <sup>25</sup> can be attributed to incorporated solvent (none noted in the previous structure vs one molecule of  $\text{CH}_2\text{Cl}_2$  in the current structure) and to the refinement differences noted in the experimental section. Unit cell parameters are slightly smaller in our structure (by 0.76% for *a* and *b* and 0.11% for *c*), but this is consistent with the lower temperature used (95 vs 203 K). Bond length esd's are 4 to 8 times smaller in our structure.

The two trans  $\text{PPh}_3$  ligands lean away from the third  $\text{PPh}_3$  ligand, with cis P–Ru–P angles of 105.8° and 99.3° and a trans P–Ru–P angle of 154.0°. The unique Ru–P bond distance of 2.505 Å is significantly longer than the trans Ru–P distances of 2.358 and 2.396 Å.

Crystals of **1-P** and **2-P<sub>2</sub>** were grown from a ternary solvent system (pentane,  $\text{CH}_2\text{Cl}_2$ , and THF) over 2–3 weeks at –78 °C. The initially white crystals turned orange upon warming, well before reaching ambient temperature. The process was not reversible, as the color remained upon recooling. Consequently, crystals of both **1-P** and **2-P<sub>2</sub>** were handled and mounted for collection of diffraction data at low temperature, but multiple problems were encountered. A successful collection was achieved for **2-P<sub>2</sub>** (Tables 1 and 2), despite strong sensitivity of the crystals not only to temperature but also to solvent loss as well as mechanical pressure.

The structure of **2-P<sub>2</sub>**, shown in Figure 4, is similar to that of  $\text{RuH}(\text{CO})\text{Cl}(\text{PPh}_3)_3$  in the arrangement of phosphine ligands. The trans  $\text{PPh}_3$  ligands again lean away from the remaining  $\text{PPh}_3$ , with cis P–Ru–P angles of 100.7° and 98.6° and a trans P–Ru–P angle of 160.0°. The trans Ru–P

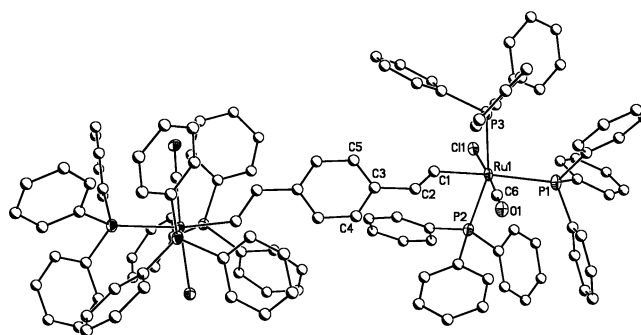


**Figure 4.** Molecular structure of **2-P<sub>2</sub>** with 30% thermal ellipsoids for non-carbon atoms. Hydrogen atoms have been omitted for clarity.

distances of 2.413 and 2.418 Å are shorter than the Ru–P (equatorial) distance of 2.552 Å.

The X-ray structure of the mononuclear osmium analogue,  $\text{Os}(\text{CO})\text{Cl}(\text{PPh}_3)_3(\text{CH}=\text{CH}-p\text{-tolyl})$ , has been reported.<sup>10</sup> Compared to this complex, the M–L distances in **2-P<sub>2</sub>** are generally slightly shorter (by 1.5% or less), but the Ru–P (equatorial) distance is longer by 2.1% (0.05 Å). The Ru complex has the trans phosphine groups angled slightly more toward the alkenyl ligand (81.4° and 80.2°) relative to the Os complex (84.2° and 83.3°).

The tilting of the trans  $\text{PPh}_3$  ligands toward the alkenyl ligand in **2-P<sub>2</sub>** is the opposite of what is seen in five-coordinate alkenyl complexes. For example, in the five-coordinate complex  $\text{Ru}(\text{CO})\text{Cl}(\text{PhC}=\text{CHPh})(\text{PPh}_3)_2$ , the P–Ru–C<sub>α</sub> (alkenyl) angles are greater than 90° (99.4° and 97.6°), averaging 17.7° greater than those in **2-P<sub>2</sub>** (81.4° and 80.2°). The adjustment of the trans  $\text{PPh}_3$  ligands upon coordination of a third  $\text{PPh}_3$  ligand is presumably responsible for the radically different coordination behavior of **2** and **3**. The longer bridge in **2** allows sufficient room for this adjustment, whereas the shorter bridge of **3** does not. A DFT geometry optimized structure of **3**<sup>26</sup> supports this view, showing the  $\text{PPh}_3$  groups on the two Ru centers to be in close proximity.

**Thermodynamic and Kinetic Analysis of the Variable Temperature NMR Spectra.** The NMR spectra of Figures 1 and 2 contain both thermodynamic information, showing a striking, temperature-dependent change in the equilibrium constant, and kinetic information, showing line-broadening and coalescence effects. Equilibrium constants might be extracted from the spectra in three ways: (1) by integration of peaks involved in slow exchange with respect to the NMR time scale (below the coalescence temperature); (2) by using the chemical shift of a fast-exchanging, averaged peak (above coalescence) to calculate the relative amounts of the contributing species; and (3) by simulation and line-shape fitting of the peaks, a method that can be applied for spectra at any temperature. Line-shape analysis also gives rate constants for the exchange processes.

The integration method was not usable for these spectra, since no peaks were observable for **1** below coalescence. In extracting equilibrium constants from chemical shifts of averaged peaks, the assumption is commonly made that the

(26) Freedman, T. B.; Sponsler, M. B. Unpublished work.

observed chemical shift is a direct weighted average of the chemical shifts of the exchanging species. However, London has shown that very large deviations from the weighted average are possible for ligand binding equilibria and that accurate calculations sometimes require inclusion of kinetic data.<sup>14</sup> Making use of rate constants from line-shape fitting (see below), we have found that the weighted-average approximation should be accurate for calculation of all averaged signals in the <sup>31</sup>P and <sup>1</sup>H spectra of Figures 1 and 2.

The weighted-average approximation was used to calculate equilibrium constants from the two averaged <sup>31</sup>P signals and from four of the five averaged styryl <sup>1</sup>H signals between 20 and -25 or -40 °C. The H<sub>α</sub> signal could not be used, since it was obscured in **1-P**. These calculations took into account the slight excess of PPh<sub>3</sub> present, and the details are given as Supporting Information. The equilibrium constants obtained from each signal were used to construct a van't Hoff plot, providing six independent determinations of  $\Delta H$  and  $\Delta S$ .

The alkenyl coupling constant,  $J_{H-H}$ , for **1**, at 13.3 Hz, differs very significantly from the value for **1-P** at 16.9 Hz.<sup>27</sup> Like the chemical shifts, the coupling constants are also averaged in the fast-exchange signals, and the large difference in this case provides another means to obtain equilibrium constants. Thus, equilibrium constants were calculated from the observed coupling constants for both alkenyl <sup>1</sup>H signals between 20 and -25 or -40 °C. From these values, two additional determinations of  $\Delta H$  and  $\Delta S$  were achieved through van't Hoff plots.

One set of <sup>31</sup>P and <sup>1</sup>H NMR spectra were recorded for each of two samples, and our analysis of chemical shifts and coupling constants therefore provided 16 independent determinations of  $\Delta H$  and  $\Delta S$ . The averages and standard deviations of these values were  $\Delta H = -17.5 \pm 2.0$  kcal/mol and  $\Delta S = -56.5 \pm 7.6$  eu. As expected for a coordination reaction, both values are negative. The equilibrium constants implied by the  $\Delta H$  and  $\Delta S$  values are 2.9 at 20 °C and  $1.7 \times 10^6$  at -70 °C. Given concentrations of **1** and PPh<sub>3</sub> of 14 and 17 mM, respectively, in the sample corresponding to Figures 1 and 2, the percent of **1** in the bound form (**1-P**) should be 4.5% at 20 °C and 99.98% at -70 °C.

As expected, the PPh<sub>3</sub> binding energy of 17.5 kcal/mol is low relative to experimental values reported for stable PPh<sub>3</sub> complexes. Ligand dissociation energies obtained from exchange reactions, requiring knowledge of another ligand dissociation energy, have been reported for PPh<sub>3</sub> complexes of Cr, Mo, and Ni, ranging from 33 to 36 kcal/mol.<sup>28</sup> A lower PPh<sub>3</sub> binding energy of 11 kcal/mol was obtained for an Ag complex by using NMR line-shape analysis.<sup>29</sup>

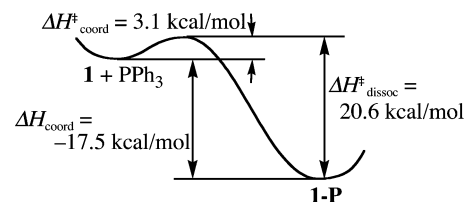


Figure 5. Enthalpy diagram for the coordination of PPh<sub>3</sub> to **1**.

Line-shape analysis was done for both the <sup>31</sup>P spectra and the five styryl hydrogens in the <sup>1</sup>H spectra. Details of the analysis are presented in Supporting Information.

Since line-shape analysis involves optimization of both thermodynamic and kinetic parameters, both van't Hoff and Eyring plots can potentially be produced. However, with both thermodynamic and kinetic parameters to be optimized and with the need for assumptions, such as temperature-independence of some of the chemical shifts (see Supporting Information for more detail), we were unable to uniquely and accurately obtain the desired parameters. Therefore, we used  $\Delta H$  and  $\Delta S$  values fixed at the average values presented above and used the simulation as a means only to obtain rate constants. With the duplicate <sup>31</sup>P and <sup>1</sup>H data sets, we obtained four independent determinations of  $\Delta H^\ddagger$  and  $\Delta S^\ddagger$  for both coordination and dissociation through Eyring plots. The average values and standard deviations were  $\Delta H^\ddagger = 3.1 \pm 0.7$  kcal/mol and  $\Delta S^\ddagger = -16.0 \pm 2.0$  for coordination and  $\Delta H^\ddagger = 20.6 \pm 0.7$  kcal/mol and  $\Delta S^\ddagger = 41.6 \pm 2.0$  eu for dissociation. The  $\Delta H^\ddagger$  and  $\Delta H$  values are combined in a potential enthalpy diagram for the reaction in Figure 5.

The activation parameters obtained are fully consistent with expectations for a coordination reaction: a low enthalpic but significant entropic barrier to coordination. In the decoordination direction, the enthalpic barrier is comparable to the ligand binding energy, with a large gain of entropy noted even at the presumably late transition state.

## Conclusions

Complexes of the type Ru(CO)Cl(PPh<sub>3</sub>)<sub>2</sub>(alkenyl) have been widely reported as stable, five-coordinate complexes. Coordination of a third PPh<sub>3</sub> ligand, though unfavorable at ambient temperature, was made to proceed for two such complexes (**1** and **2**) with very high equilibrium constants by lowering the temperature by 75–90 °C. From dynamic NMR data that simultaneously showed a strong equilibrium shift and coalescence, we were able to obtain both thermodynamic and kinetic parameters for the ligand binding to **1**, giving a complete energy profile for the coordination/decoordination process. Whereas coordination of PPh<sub>3</sub> to the dinuclear complex **2**, with a CH=CHC<sub>6</sub>H<sub>4</sub>CH=CH bridge, was observed at low temperature, the shorter complex **3**, with a CH=CHCH=CH bridge, showed no signs of such coordination.

**Acknowledgment.** We thank the donors of The Petroleum Research Fund, administered by the American Chemical Society, for support of this research. This work was also supported by the National Science Foundation under Grant No. CHE-0320583. We also gratefully acknowledge funds

(27) The value for **1** was the same at 20 and -70 °C, while the value for **1-P** could only be measured at -70 °C. The latter was assumed to be temperature-independent.

(28) Dias, P. B.; Minas de Piedade, M. E.; Simoes, J. A. M. *Coord. Chem. Rev.* **1994**, *135/136*, 737–807.

(29) Carmona, D.; Ferrer, J.; Lamata, M. P.; Oro, L. A.; Limbach, H. H.; Scherer, G.; Elguero, J.; Jimena, M. L. *J. Organomet. Chem.* **1994**, *470*, 271–274.

*Coordination to Alkenylruthenium Complexes*

from the NSF (CHE-9527898), the W. H. Keck Foundation, and Syracuse University, which made possible the purchase of the X-ray diffractometer. We thank Jacob Alexander and Weijie Teng for data-handling assistance with the X-ray results, David J. Kiemle for collection of the NMR data, and Professor Alex D. Bain, McMaster University, for helpful correspondence.

**Supporting Information Available:** NMR data and analysis methods, thermodynamic and kinetic results for the coordination of  $\text{PPh}_3$  to **1**, and X-ray crystallographic data for  $\text{RuH}(\text{CO})\text{Cl}(\text{PPh}_3)_3$  and **2-P<sub>2</sub>**. This material is available free of charge via the Internet at <http://pubs.acs.org>.

IC061389F